Design and control of a novel asymmetrical piezoelectric actuated microgripper for micromanipulation

Cunman Liang, Fujun Wang*, Yanling Tian, Xingyu Zhao, and Dawei Zhang

Key Laboratory of Mechanism Theory and Equipment Design of Ministry of Education, School of Mechanical Engineering, Tianjin University, Tianjin 300072, China

Abstract: Microgripper is an important tool in high precision micromanipulation task, which directly affects the quality and efficiency of micromanipulation. This paper presents the design and control of a novel asymmetrical microgripper driven by a piezoelectric (PZT) actuator. The developed microgripper is designed as an asymmetrical structure with just one movable jaw, so it has the advantages of no dense mode and fixed locating datum compared with the symmetrical microgripper with two movable jaws. The main body of microgripper is a compact flexure-based mechanical structure with a three-stage amplification mechanism. Based on the designed structure, large-range, robust and parallel grasping operation can be realized. The characteristics analyses of the developed microgripper are carried out by finite element analysis (FEA). A position-force switching control strategy is utilized to regulate the position and grasping force of movable jaw. Discrete-time sliding model controller (DSMC) is designed to control the position and grasping force of grasping jaw. Experimental studies are conducted and the results show that the microgripper exhibits good performance and high precision grasping operations can be realized through the developed control strategy.

Keywords: Microgripper, Flexure mechanism, Mechanical design, Position-force control

*Corresponding author: Fujun Wang, Key Laboratory of Mechanism Theory and Equipment Design of Ministry of Education, School of Mechanical Engineering, Tianjin University, Tianjin 300072, China. Email: wangfujun@tju.edu.cn. Tel/fax: 86-022-27405561.

1. INTRODUCTION

Recently, the demands of micromanipulation in terms of precision and efficiency have been growing with the development of biological engineering, microelectronics industry et.al [1-3]. As the operated objects in micromanipulation are developing toward ultra-micronization, the difficulty of micromanipulation is increasing continuously. Microgripper, as a key component of precision micromanipulation systems, plays an important role during the operation process [4, 5]. The microgripper contacts the operated objects directly in the automated grasp-hold-release operations, so the performance of microgripper will directly affect the quality, efficiency and accuracy of micromanipulation [6-7].

Nowadays various types of microgrippers have been developed according to different actuations, such as electrothermal, coil voice actuated, shape memory alloy (SMA) actuated and piezoelectric (PZT) microgrippers [8-11]. Particularly PZT actuator has the advantages of small volume, large output force, fast response and zero backlash, so it has been widely used in microgripper [12-14]. Since the output displacement of PZT actuator is quite small which is usually several tens micrometers, displacement amplification mechanism (DAM) has an important effect on the PZT-actuated microgripper which is utilized to amplify the output displacement of actuator and transmit the displacement from the actuator to the jaws. Based on different types of DAMs several PZT-actuated microgrippers have been developed. Sun et al. designed a PZT driven compliant-based microgripper for micromanipulation which consists of Scott-Russell mechanism and leverage mechanism [15]. Xu designed a PZT-actuated microgripper with a two-stage flexure-based DAM [16]. Wang et al. designed a

monolithic compliant PZT driven microgripper with a larger displacement amplification ratio [17]. Zubir et al. designed an asymmetrical PZT driven microgripper with two grasping jaws movable to obtain large range of grasping operation [18]. Most present PZT actuated microgrippers are designed with two movable grasping jaws. The advantage of this kind microgripper is that large displacement amplification ratio can be realized which can meet the requirement of grasping large scale objects. However, the inevitable error during fabrication and assembly may lead to asymmetric motion of movable jaws, which will make the grasping objects not in the center line of the jaws. Therefore the operation precision will be reduced inevitably. In addition the first two mode shapes of the microgripper with two jaws movable are usually too close to each other. The dense modes will lead bad dynamic characteristics and bring troubles to the control of microgripper. The microgripper with one movable jaw has a specific and fixed locating datum which can improve the operation accuracy. Moreover, since just one grasping jaw is movable, only one side of the microgrippers is flexible. Therefore there is no dense modes problem in the asymmetrical microgrippers with one movable jaw.

For the reason that the micro-objects are usually small and easily broken, both precise position and stable grasping force are required to be guaranteed during micromanipulation process. Therefore high performance position-force controller is needed during working process. Unfortunately, most of the present microgrippers focus on position control and the researches dedicate to both position and grasping force control are relatively rare to find. There are several effective and practical control methodologies in terms of position and force control, including hybrid control [19, 20], impedance control [21, 22] and switching control [23, 24]. Hybrid control and impedance control are

applicable to the system that the force and the position are coupled, while the switching control is suitable to the force and position decoupled control system. Compared with the other control methodologies the switching control has a concise structure and is easy to implement, especially in force and position decoupled control system. As the most common controller, proportional-integral-derivative (PID) controllers are the most dominating form of feedback in use today [25]. But due to the high-frequency dynamic vibrations during the fast grasping and releasing operations, traditional PID control can not satisfy the requirement of precision position-force regulation. To overcome this problem, several advanced controllers including the adaptive robust control [26], iterative learning control [27] and neural networks control [28] et.al, are proposed to control precision positioning systems. However expensive algorithms and calculations, together with complex parameters tuning process make the applications of these controllers limited. Since the discrete-time sliding mode controller (DSMC) has the advantages of fast response and strong robustness, DSMC becomes one of the most promising candidates for the control of microgrippers.

This paper is motivated to design a novel high performance microgripper, which is designed asymmetrically with one movable jaw. Through the flexure-based mechanical structure with a three-stage amplification mechanism, the input displacement can be amplified and parallel jaw grasping can be realized. The characteristic analyses of the developed microgripper are carried out based on finite element analysis (FEA). A position-force switching control strategy composed of position and force DSMCs is utilized to realize the position and force control of the developed microgripper. Finally

the microgripper is fabricated and corresponding experimental tests are carried out to investigate its performance.

2. STRUCTURE DESIGN

Figure 1 illustrates the mechanism of the designed microgripper, which consists of a PZT actuator, a fixed jaw, a moveable jaw, a flexible beam, a preload bolt, a base and a flexible DAM. The flexible DAM is designed as a three-stage amplification mechanism which consists of a leverage mechanism, a bridge-type mechanism and a parallelogram leverage mechanism. The PZT actuator is installed between the base and the leverage mechanism by the preload bolt at one end of the PZT actuator; the preload force applied on the PZT actuator can be adjusted by the bolt. The microgripper is designed asymmetrically with just one side of the microgripper flexible. The fixed jaw is fixed to the base while the moveable jaw is connected with the DAM through a flexible beam. A stain gage is glued on the base end of the flexible beam to measure the grasping force applied on the manipulated micro-object. The geometry and parameters of the developed microgripper is shown in Fig. 2. The main parameters are determined by several iterations of design and simulation, which is shown in Tab. 1.

Due to the output displacement of the PZT actuator is very small, the microgripper should have enough large displacement range to grasp different sizes of micro-objects; thus a flexure-based DAM with large amplification ratio is designed. The motion transmission from the PZT actuator to the moveable jaw is realized through the DAM, while the output displacement of the PZT actuator is magnified. As the first-stage amplification the leverage mechanism can amplify the output displacement of the PZT

actuator based on the deformation of flexure hinge as shown in Fig. 3(a). The bridge-type mechanism is designed as the second-stage amplification which consists of a connecting rod mechanism connected by four elliptical flexure hinges. The working principle of the bridge-type mechanism is that once driven by an input displacement, the device produces a vertical output displacement as shown in Fig. 3(b). The parallelogram mechanism shown in Fig. 3(c) can work like a leverage mechanism which is the third-stage amplification. Moreover pure jaw translations of moveable jaw can be realized based on the parallelogram mechanism, which can guarantee stable and robust grasping manipulations.

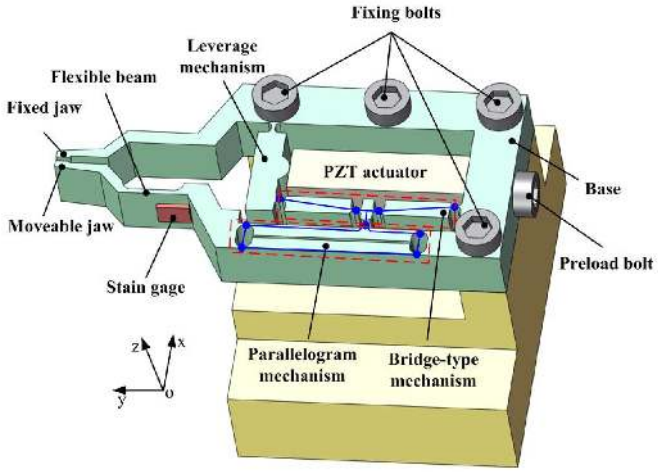

Fig. 1 Mechanism of the developed microgripper.

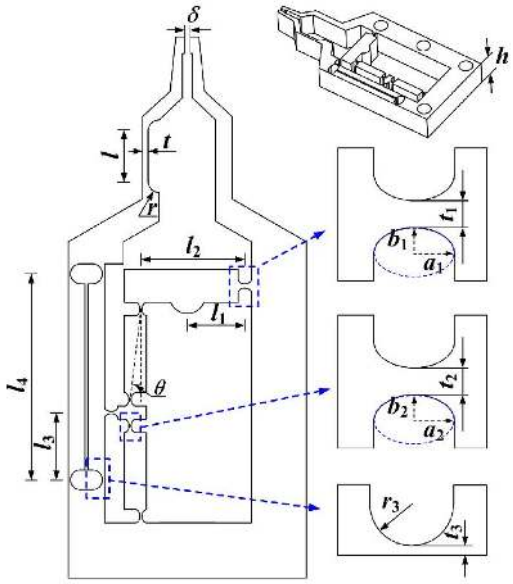

Fig. 2 Geometry and parameters of the developed microgripper.

Tab. 1 Dominant parameters of the microgripper.

Symbol	Value	Symbol	Value	Symbol	Value
l_1	5.2 mm	b_1	0.4 mm	t_3	0.2 mm
l_2	9.4 mm	t_1	0.4 mm	l	4.6 mm
l_3	6.1 mm	a_2	0.6 mm	t	0.5 mm
l_4	18.7 mm	b_2	0.4 mm	r	1 mm
θ	7°	t_2	0.2 mm	δ	0.5 mm
a_1	0.6 mm	r_3	0.9 mm	h	6 mm

During the working process, the PZT actuator will expand and push the leverage mechanism; then the leverage mechanism will swing upward and pull the bridge-type mechanism; finally the parallelogram mechanism pulled by the bridge-type mechanism will swing and cause the moveable gripping jaw to close to grasp the manipulated

micro-object. After power is switched off, the PZT actuator will retract to its original length and the flexible motion transmission mechanism will return to its initial position, which causes the moveable grasping jaws to release the micro-object.

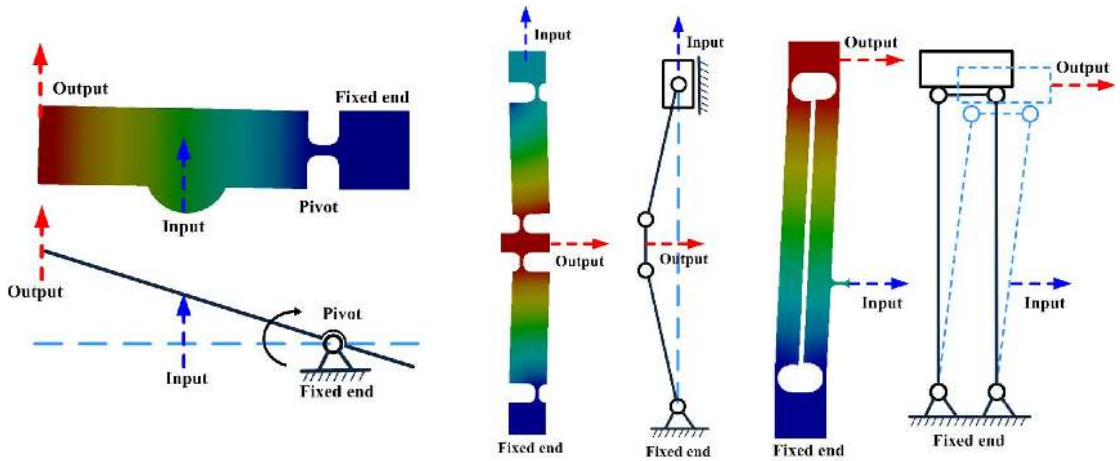

(a) **(b)** **(c)**

Fig. 3. Working principle of amplifications: (a) leverage mechanism, (b) bridge-type mechanism and (c) parallelogram mechanism.

Fig. 4. Grasping mode: (a) one movable jaw and (b) two movable jaws.

One advantage of the designed asymmetrical microgripper with just one movable jaw is that it has a specific and fixed locating datum as shown in Fig. 4(a). The locating

datum of the symmetrical microgripper with two jaws movable may not be fixed and has a drift due to the inevitable error during microgripper fabrication and assembly as shown in Fig. 4(b). Therefore the asymmetrical microgripper with one movable jaw is more suitable for application of high precision micromanipulation, such as high precision micro assembly.

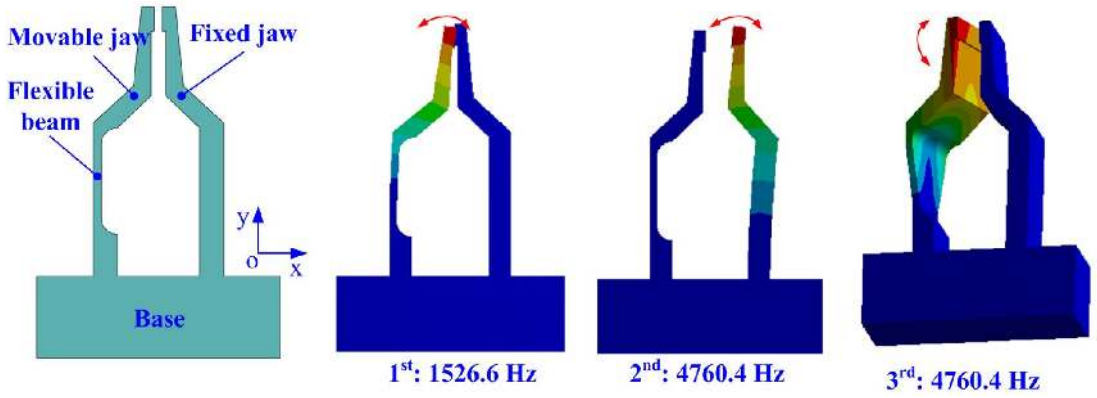

(a)

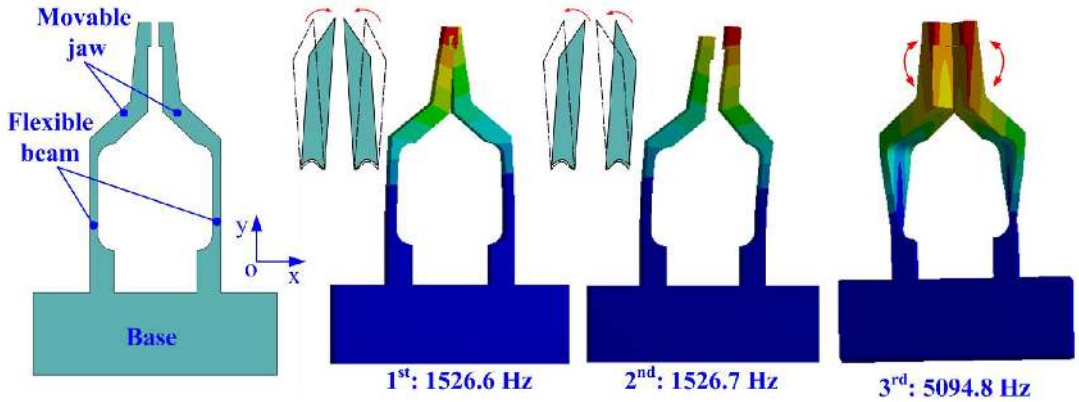

(b)

Fig. 5. Dynamic performances of two type microgrippers: (a) asymmetrical microgripper and (b) symmetrical microgripper.

Another advantage of the designed asymmetrical microgripper with one movable jaw is that it has no dense modes and better dynamic performance. Figure 5 shows the

comparison of the two type microgrippers in term of the natural frequency and mode shape where the microgrippers are the simplified models with jaws, flexible beam and base. The flexible beam presents the flexible mechanism which transfers the motion from the actuator to the jaws. The dynamic performances of two type microgrippers are investigated by finite element analysis (FEA) with the material properties and boundary conditions. The first three mode shapes and corresponding natural frequencies of each type microgripper are obtained and shown in Fig. 5. The first mode shape of symmetrical microgripper is that the jaws vibrate in the opposite directions and the second mode shape is that the jaws vibrate in the same direction. However the frequencies of first two modes are too close to each other, which will increase the difficulty of the control of microgripper. The frequencies of first two modes of microgripper designed asymmetrically with one jaw movable are no longer close to each other. From the result we can find that the dynamic characteristics of microgripper designed asymmetrically with one movable jaw are better than those of the symmetrical microgripper. Therefore the asymmetrical microgripper is more suitable for application in high frequency micromanipulation, such as wire grasping in wire bonder.

3. CHARACTERISTIC ANALYSIS

In order to investigate the characteristics of the designed microgripper, FEA is carried out with the aid of ANSYS software. The finite element model is established with 20-node element SOLID186. Zero displacements are assigned on the surfaces of the two fixing holes during simulation. Input displacement of 10 μm is applied on the input terminal of the microgripper for the static analysis, since the maximum output

displacement of the PZT actuator is assumed as 10 μm in working condition. The deformation behavior and stress distribution of the microgripper is shown in Fig. 6. The maximum displacement of the moveable jaw can reach 149.4 μm, so the displacement amplification ratio of the microgripper can be calculated as 14.94. The evaluation of parallel movement is obtained; the x-axis displacements of the movable jaw, flexible beam and output terminal of the parallelogram mechanism are almost the same, which are between 146.9 μm and 149.4 μm while the relative error is 1.67%. It should be pointed out that the displacement of output terminal of the parallelogram mechanism is larger than that of the movable jaw. The reason is that the force applied on the input terminal of parallelogram mechanism is not just in x-axis direction which is also has a component in y-axis direction. The parasitic displacements in y-axis of the movable jaw, flexible beam and output terminal of parallelogram mechanism are also obtained which is shown in Fig. 6(a). The maximum parasitic error is located in the movable jaw which is 1.47μm and the maximum relative parasitic error is 0.98%. Moreover the results also show that the maximum stress occurs at the flexure hinge which connects the bridge-type mechanism and the parallelogram mechanism. The maximum stress is 198.9MPa, which is far less than the yield strength (503 MPa) of the material of the microgripper, AL7075-T651.

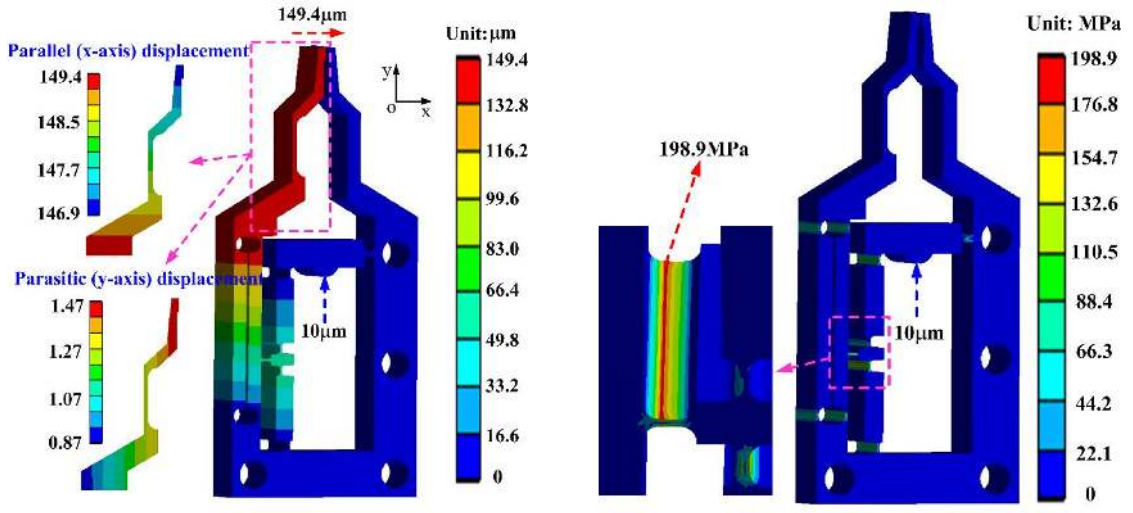

(a) **(b)**

Fig. 6. Static analysis results by FEA: (a) deformation behavior; (b) stress distribution.

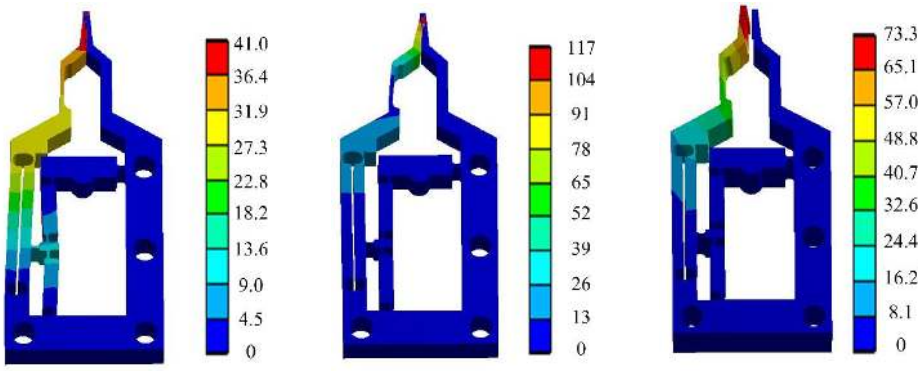

(a) **(b)** **(c)**

Fig. 7. First three mode shapes of the microgripper: (a) 575 Hz, (b) 1560 Hz and (c) 2360 Hz.

Besides, the modal analysis is performed to investigate the dynamic performance of the microgripper. Based on the modal analysis the first three natural frequencies and corresponding mode shapes are obtained and shown in Fig. 7. The first mode shape of the microgripper is that the moveable jaw and the parallelogram mechanism vibrate in x-axis direction which is consistent with the working state, and the corresponding natural frequency is 575 Hz. The second mode shape shows the moveable jaw vibrates in x-axis

direction around the flexible beam and the corresponding natural frequency is 1560 Hz. In the third mode shape the flexible beam and the movable jaw swing up and down; the corresponding natural frequency is 2360 Hz. From the results of model analysis it can be found that there is no dense mode between the first two modes. Therefore the microgripper exhibits good dynamic performance.

4. CONTROLLER DESIGN

4.1 PID-type DSMC

Considering that there may be hysteresis in the control of piezoelectric actuated system, discrete-time sliding mode control (DSMC) which has strong robustness has been adopted for the position and force control. The DSMC with PID-type sliding surface offers a faster transient response and less steady-state error compared with the traditional DSMC featured with PD-type sliding surface. Hence, DSMC with PID-type sliding surface is utilized for the control of the designed microgripper.

It is known that the transfer functions of position response can be represented as:

$$x(k) = \sum_{i=1}^{n} a_i x(k-i) + \sum_{i=0}^{m} b_i u(k-i) + p(k) \tag{1}$$

where a_i and b_i are the coefficients and $x(k)$ and $u(k)$ present output position and input voltage at time step k, respectively. In addition, $p(k)$ is perturbation which includes piezoelectric hysteresis, drift, external force, parameter uncertainties, and other model disturbances.

The perturbation can be estimated by

$$p^*(k) = p(k-1) = x(k-1) - \sum_{i=1}^{n} a_i x(k-1-i) + \sum_{i=0}^{m} b_i u(k-1-i) \tag{2}$$

Then the dynamic model of Eq. (1) can be expressed as

$$x(k) = \sum_{i=1}^{n} a_i x(k-i) + \sum_{i=0}^{m} b_i u(k-i) + p^*(k) + p_e(k) \tag{3}$$

where $p_e(k) = p(k) - p^*(k)$ represents the error between the estimated perturbation and real perturbation.

It can be deduced that $p_e(k)$ is also bounded

$$\left|p_e(k)\right| = \left|p(k) - p^*(k)\right| = \left|p(k) - p(k-1)\right| \le \kappa T_s \tag{4}$$

where κ is a positive constant and T_s is the sampling time.

In this paper, the output tracking error is defined as follows:

$$e(k) = x(k) - x_r(k) \tag{5}$$

where $x_r(k)$ is the desired output.

Based on the error in Eq (5), the PID-type sliding function is defined as follows:

$$s(k) = c_1 e(k) + c_2 \varepsilon(k) + e(k) - e(k-1) \tag{6}$$

where c_1 and c_2 are positive parameters.

In addition, the integral error item $\varepsilon(k)$ is defined as

$$\varepsilon(k) = \sum_{i=1}^{k} e(i) = \varepsilon(k-1) + e(k) \tag{7}$$

Designing the sliding control law as

$$u(k) = -\frac{1}{b_0}\left(\sum_{i=1}^{n} a_i x(k-i) + \sum_{i=1}^{m} b_i u(k-i) + p^*(k) - x_r(k)\right) + \frac{(c_1+2)e(k-1) - e(k-2)}{cb_0} + slaw \tag{8}$$

where $slaw = -\frac{1}{b_0}\left(\lambda_1 T_s s(k-1) + \lambda_2 T_s \operatorname{sgn}(s(k))\right)$, λ_1 and λ_2 are positive constant parameters, $c=c_1+c_2+1$ and sgn is sign function.

Substituting Eq. (8) into Eq. (3), the following equation can be obtained:

$$x(k) = x_r(k) + p_e(k) + \frac{c_1 + 2}{c} e(k-1) - \frac{1}{c} e(k-2) - \lambda_1 T_s s(k-1) - \lambda_2 T_s \operatorname{sgn}(s(k-1)) \quad (9)$$

Substituting Eq. (9) into the equation of PID-type sliding function (6) yields

$$\begin{aligned} s(k) &= c_1 e(k) + c_2 \varepsilon(k) + e(k) - e(k-1) \\ &= s(k-1) + c_1 \big(e(k) - e(k-1)\big) + c_2 e(k) + e(k) - 2e(k-1) + e(k-2) \\ &= s(k-1) + ce(k) - (c_1+2) e(k-1) + e(k-2) \\ &= s(k-1) + c\big(p_e(k) - \lambda_1 T_s s(k-1) - \lambda_2 T_s \operatorname{sgn}(s(k-1))\big) \end{aligned} \quad (10)$$

To evaluate the stability of the control system, a Lyapunov function is defined as

$$V(k-1) = \frac{1}{2} s^2(k-1) \quad (11)$$

The following conditions should be satisfied:

$$\Delta V(k-1) = s^2(k) - s^2(k-1) < 0 \quad (12)$$

Since the sampling time is short, Eq. (12) can be written as

$$\begin{cases} \big(s(k) - s(k-1)\big)\operatorname{sgn}\big(s(k-1)\big) < 0 \\ \big(s(k) + s(k-1)\big)\operatorname{sgn}\big(s(k-1)\big) > 0 \end{cases} \quad (13)$$

For the DSMC with the exponential reaching law, the following relationship can be deduced:

$$\begin{aligned} &\big(s(k) - s(k-1)\big)\operatorname{sgn}\big(s(k-1)\big) \\ &= c\big(p_e(k) - \lambda_1 T_s s(k-1) - \lambda_2 T_s \operatorname{sgn}\big(s(k-1)\big)\big)\operatorname{sgn}\big(s(k-1)\big) \\ &= c\big(p_e(k)\operatorname{sgn}\big(s(k-1)\big) - \lambda_1 T_s \big|s(k-1)\big| - \lambda_2 T_s\big) \\ &\le c\big((\kappa - \lambda_2) T_s - \lambda_1 T_s \big|s(k-1)\big|\big) \end{aligned} \quad (14)$$

If the gain λ_2 is designed to meet the condition $\lambda_2 > \kappa + o$, where o is an arbitrary positive constant, the following relationship can be obtained:

$$\begin{aligned} \big(s(k) - s(k-1)\big)\operatorname{sgn}\big(s(k-1)\big) &\le c\big((\kappa - \lambda_2) T_s - \lambda_1 T_s \big|s(k-1)\big|\big) \\ &< c\big(-oT_s - \lambda_1 T_s \big|s(k-1)\big|\big) < 0 \end{aligned} \quad (15)$$

When the sampling time T_s is short, the following relationship can be obtained:

$$
\begin{aligned}
&\big(s(k)+s(k-1)\big)\mathrm{sgn}\big(s(k-1)\big)\\
&=\big(s(k-1)+cp_e(k)-c\lambda_1 T_s s(k-1)-c\lambda_2 T_s\,\mathrm{sgn}\big(s(k-1)\big)\big)\mathrm{sgn}\big(s(k-1)\big)\\
&=cp_e(k)\,\mathrm{sgn}\big(s(k-1)\big)+(2-c\lambda_1 T_s)\big|s(k-1)\big|-c\lambda_2 T_s\\
&\geq -c(\kappa+\lambda_2)T_s+(2-c\lambda_1 T_s)\big|s(k-1)\big|>0
\end{aligned}
\tag{16}
$$

Based on Eq. (15) and (16), the system can be verified to be stable.

4.2 Position-force switching control strategy

The grasping task of microgripper can be classified into three phases, namely the closing phase, contact phase and opening phase. In closing and opening phases position control is essential to ensure high position precision of moveable jaw, while in contact phase force control is required to make the grasping force controllable. Therefore a position-force control strategy is utilized in which the final voltage in previous phase should be the base value for the next phase to guarantee a stable and smooth transition. Once the moveable jaw contacts the object and the grasping force exceeds the threshold value, the control system switches to the force control from the position control. When it is time to release the object, the control system will switch to the position control again. The flow chart of the position-force switching control strategy is shown in Fig. 8. In the flow chart F_r is the desired grasping force of force control in contact phase, while d_{r1} and d_{r2} are the desired displacements of position control in closing phase and opening phase, respectively. F_s is the threshold force, t_g is the time to release the object and T_g is overall time of grasping operation. u_{sp} is the switching voltage from position control to force control and u_{sf} is the switching voltage from force control to position control.

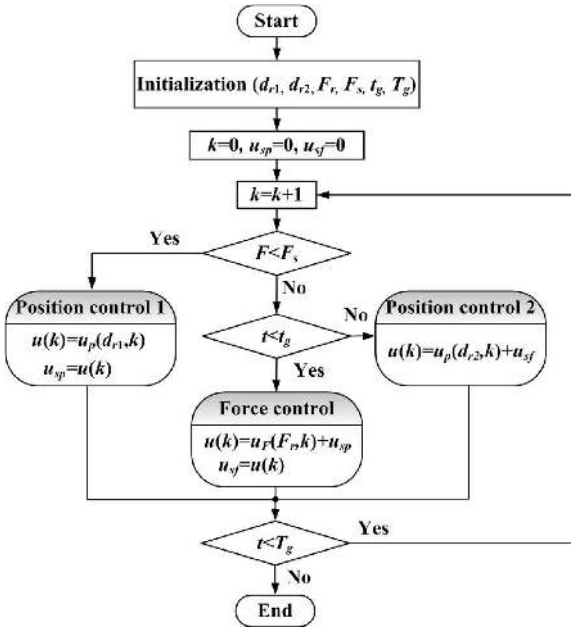

Fig. 8. Flow chart of the position-force switching control strategy.

5. EXPERIMENTS

5.1 **Prototype development and experimental setup**

In order to guarantee the geometrical accuracy wire electro-discharge machining (WEDM) technique is utilized to manufacture the flexure-based mechanism. Figure 9 shows the prototype of microgripper made by AL7075-T651. AL7075-T651 has the property of high elasticity, yield strength, and light mass for the excellent physical and thermal properties. The initial gap between the grasping jaws can be adjustable by the preload bolt to grasping different sizes of objects.

Fig. 9. Prototype of the microgripper.

A number of tests have been conducted on the designed microgripper which is mounted on a vibration-isolated Newport RS-4000 optical table to reduce the external vibration disturbance. Two laser displacement sensors, which provide a 50 nm resolution within a 20 mm measuring range, are employed to measure the input displacement and output displacement of the microgripper, respectively. As shown in Fig. 10 (a) the input displacement is measured at the point where the PZT actuator pushes the leverage mechanism and the output displacement is measured at the point on the output terminal of the parallelogram leverage mechanism. For the purpose to measure the grasping force a strain gage is glued on the on the base end of the flexible beam, which is adopted form a quarter Wheatstone bridge for the grasping force measurement. A dynamic strain gauge system is adopted to measure the signal of Wheatstone bridge. The strain gage is calibrated by hanging several objects on the movable jaw, whose weights are measured by electronic balance. At the same time the output voltage of the sensor are acquired by NI data acquisition card. The gain is then calculated as 0.559 mN/mV, which is used to

convert the voltage into force value. A dSPACE DS1103 controller is adopted to implement the control algorithm, which picks up the displacement and force signals to determine the current state of the microgripper. In addition, a voltage amplifier (E505.00 from PI, Inc) is utilized to amplify the output voltage of controller for the PZT actuator drive and the gain factor is 10. All the devices are also placed on the vibration-isolated table and experimental setup is displayed in Fig. 10 (b).

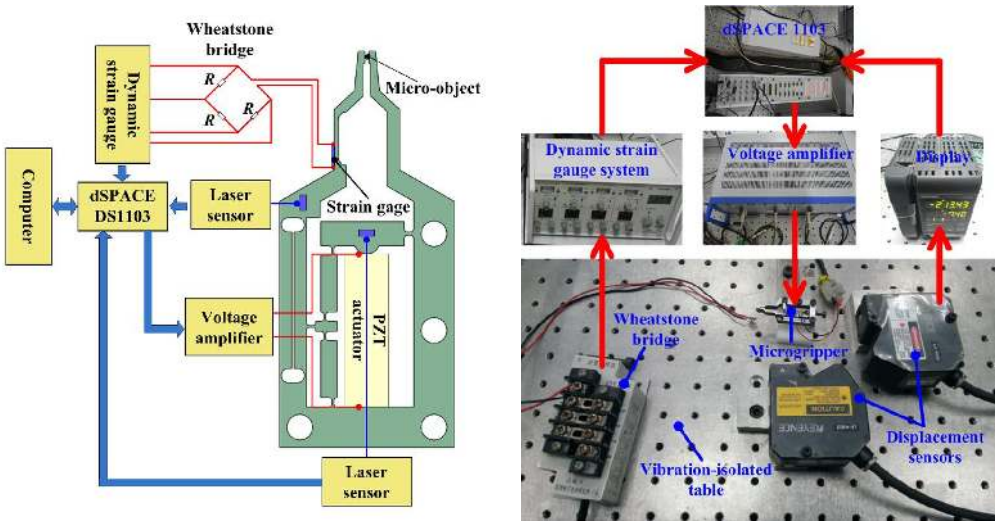

(a) **(b)**

Fig. 10. Experimental setup: (a) schematic diagram and (b) photograph.

5.2 Characteristics test

In order to measure the displacement amplification ratio, a sinusoidal signal with the amplitude of 60 V and frequency of 1 Hz is applied on the PZT actuator. The input and output displacements can be measured by two laser displacement sensors at the same time; therefore the relationship between the input and output displacements can be obtained. Figure 11 shows that the experimental measured displacement amplification ratio is 13.94,

while the displacement amplification ratio of simulation is 14.94. It is can be seen that the result of experiment is in good agreement with the result of simulation.

The dynamic characteristics of the microgripper are examined by means of frequency response. In order to obtain the experimental data swept sine waves with the amplitude of 0.6 V and frequency range of 0.1 - 1200 Hz are applied on the PZT actuator through the voltage amplifier, which are produced by dSPACE DS1103 controller. The position response is measured by the laser displacement sensor while the microgrpper is operated freely, and the force response is measured by the strain gage while a 25.4-μm gold wire is selected as a grasped object to identify force model. The output signals of position and force responses are acquired within 10 kHz and then the Matlab System Identification Toolbox is used to process the data. The results are summarized in Fig. 12. In Fig. 12(a) a resonant peak in position response at the frequency of 531 Hz is observed, which is 8.3% lower than the value (575 Hz) predicted by FEA simulation. Based on the experimental data the transfer functions of position and force are achieved from the input-output sequences, which are given as

$$G_P(z) = \frac{-3.911z^3 + 13.11z^2 - 15.34z + 6.275}{z^3 - 2.719z^2 + 2.567z - 0.83} \tag{17}$$

$$G_F(z) = \frac{-0.009302\,z + 0.01923}{z^2 - 1.733z + 0.9854} \tag{18}$$

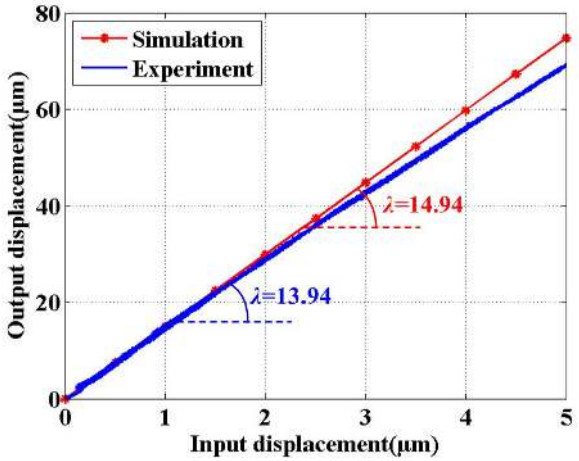

Fig. 11. Relationship between the input and output displacements.

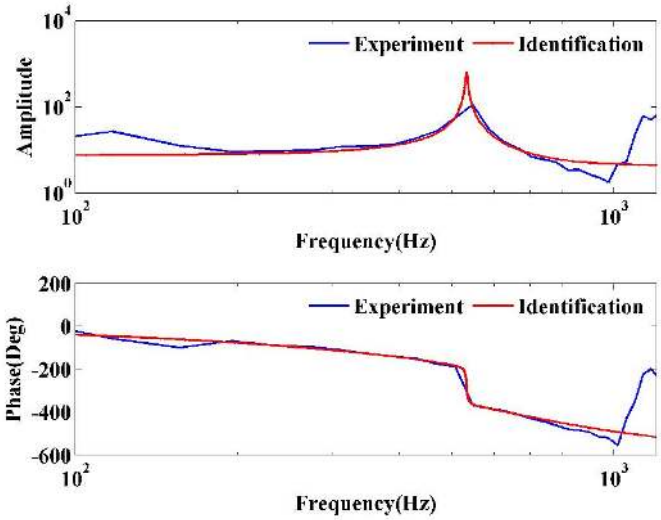

(a)

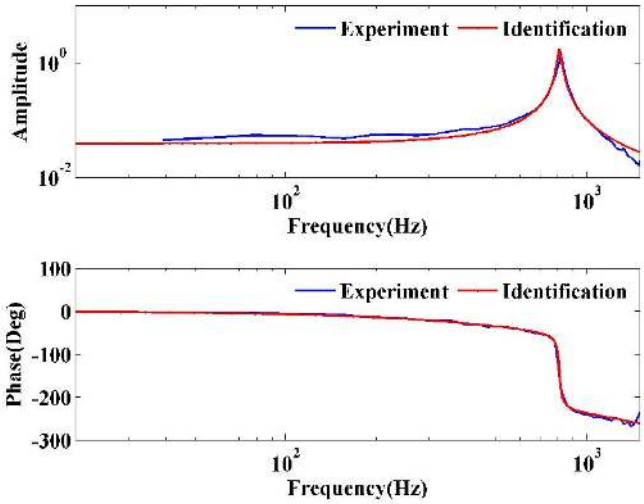

(b)

Fig. 12. Results of system identification: (a) position response and (b) force response.

5.3 Control experiment

Several control experiments are carried out to examine the performance of the designed controller. During the experiments, gold wires with a diameter of 25.4 μm are employed to verify the effectiveness of the switching control strategy.

Step response is investigated and the desired displacement trajectory is defined as a step signal with a final value as 20 μm. The result of step response by position control is shown in Fig. 13. From the result it can be seen that the settling time is 12 ms, the overshoot is 2.5%, and the steady-state error is ±0.2 μm. The sinusoidal response is investigated using a sinusoidal reference input with the amplitude of 10 μm, frequency of 20 Hz and bias of 10 μm, which is shown in Fig. 14(a). The corresponding position tracking errors are illustrated in Fig. 14(b). It is found that the tracking errors are within ±1.3 μm.

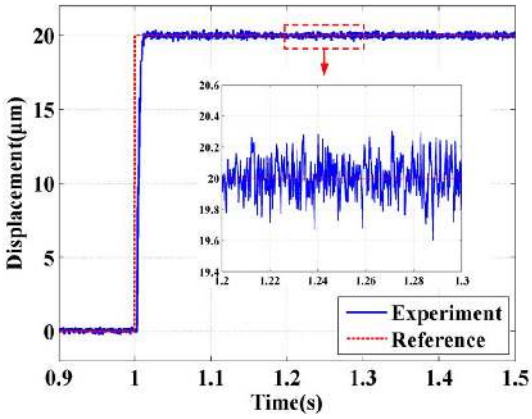

Fig. 13. Displacement step response of the microgripper.

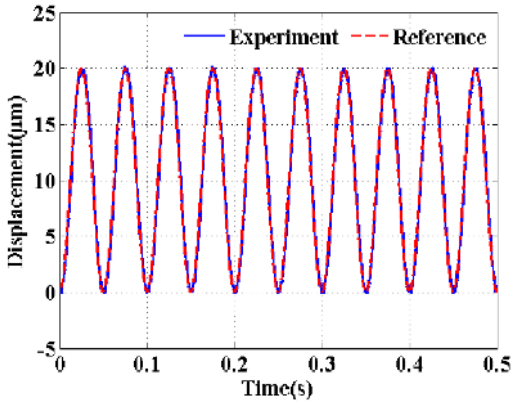

(a)

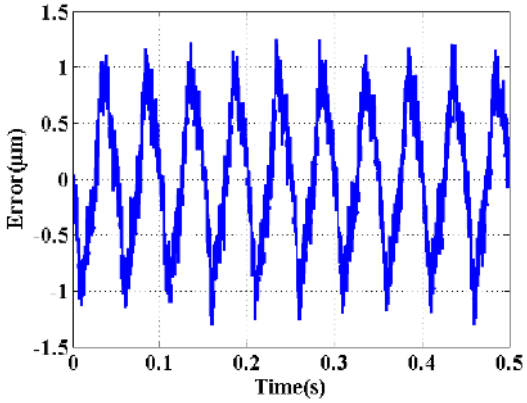

(b)

Fig. 14. Displacement sinusoidal response of the microgripper: (a) displacement and (b) displacement error.

In order to verify the performance of the force controller, step response with a final value as 50 mN is investigated while the threshold force is set as 5 mN. The results are shown in Fig.15. From the results it can be seen that the settling time is 30 ms, the overshoot is 1.3%, and the steady-state error is ±0.4 mN.

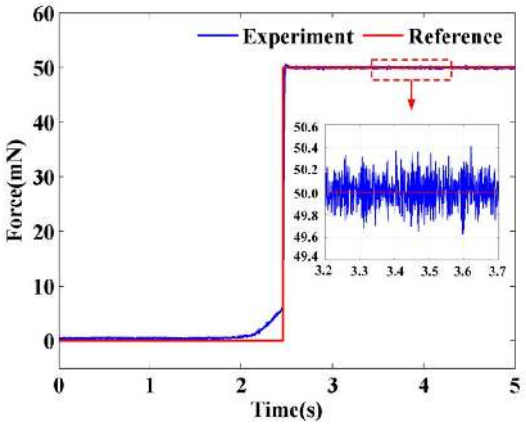

Fig. 15. Force step response of the microgripper.

For the purpose to achieve a complete and efficient grasp-hold-release operation, the position and force trajectories are planned as shown in Fig.16. In order to ensure smooth switching, fast close and slow contact is essential in closing phase, a homothetic trapezoidal velocity planning is employed to control the jaw displacement which leads to the contact of the jaws and grasped wire with a constant velocity. In the contact phase a step force signal is utilized as the reference signal of the grasping force. In order to make the jaw return to its initial position, the trapezoidal velocity planning is used based on the final position in the contact phase.

Figure 17 shows the results of position-force switching control in the grasp-hold-release operation. The results show that the steady-state error of grasping force is ±0.4 mN, the settling time is 20 ms and the overall time of the operation is

within 180 ms. The comparison with other similar works is conducted and shown in Tab. 2. We can find that the developed microgripper outperforms the others in terms of no dense mode, and faster overall operation time.

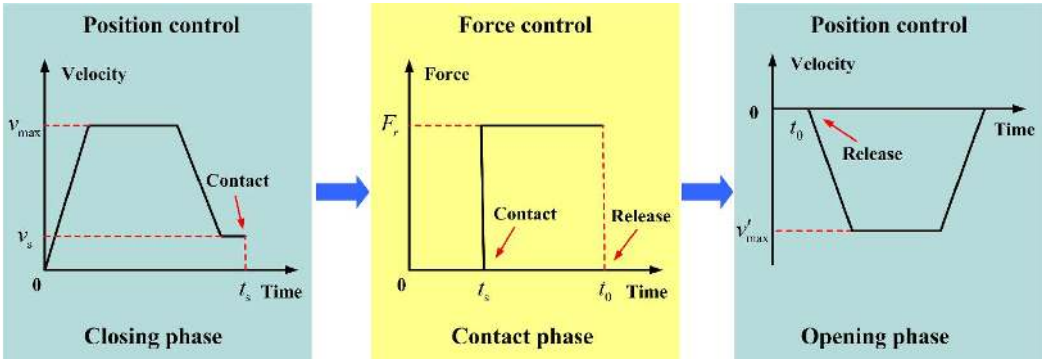

Fig. 16. Trajectory planning of position and force control.

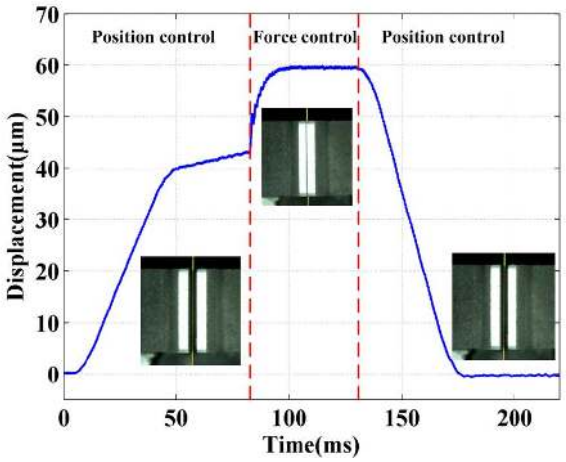

(a)

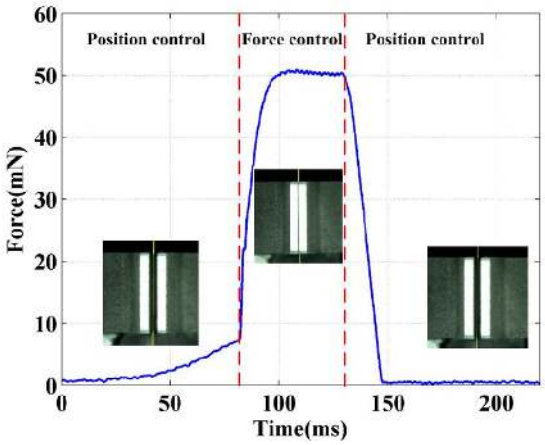

(b)

Fig. 17. Results of position-force switching control in the grasp-hold-release operation: (a) displacement response, and (b) force response.

Tab. 2 Comparison with other microgrippers.

Actuation	First vibration frequency	Second vibration frequency	Overall operation time	Position/force control	Reference
Thermo-Piezoelectric	667 Hz	-	120s	Yes	[6]
Voice coil motor	-	-	>1s	No	[9]
PZT	842 Hz	986 Hz	-	No	[11]
PZT	359.56 Hz	-	>12s	No	[17]
PZT	141.67 Hz	150.44 Hz	20s	No	[29]
PZT	244 Hz	-	>5s	Yes	[24]
PZT	1062 Hz	1344 Hz	-	No	[30]
PZT	575 Hz	1560 Hz	0.18s	Yes	This works

6. CONCLUSION

A novel piezoelectric actuated microgripper has been reported in this paper, which is designed asymmetrically with just one jaw movable. Through a three-stage flexure-based mechanical structure a large displacement amplification ratio has been achieved. The designed microgripper has the advantages of no dense mode and fixed locating datum compared with the symmetrical microgripper with two movable jaws. The characteristics analyses of the developed microgripper are carried out based on FEA. A position-force switching controller has been designed, which is composed of position and force controllers and DSMC is utilized in the position and force controller. The designed microgripper has been manufactured through WEDM technique. Experimental tests have been implemented to examine the performance of the microgripper. The results show that the amplification ratio of the designed microgripper is 13.94 and the mode frequency is 531 Hz, which are in good agreement with the results by simulation. The performance of microgripper by executing grasping operations of gold wire has been tested with the position-force switching controller. The position step response show that the settling time is 12 ms, the overshoot is 2.5%, and the steady-state error is ±0.2 μm. For the force step response, the settling time is 30 ms, the overshoot is 1.3%, and the steady-state error is ±0.4 mN. With position-force trajectory plan, fast and robust grasping operations have been achieved, and the results show that the steady-state error of grasping force is ±0.4 mN, the settling time is 20 ms and the overall time of the operation is within 180 ms. The experimental results indicate that microgripper exhibits good performance and high precision grasping operations can be realized through the developed control strategy.

ACKNOWLEDGMENTS

This work was supported by the National Natural Science Foundation of China (Grant nos.51675376 and 51205279), the Science & Technology Commission of Tianjin Municipality (Grant no. 13JCQNJC04100), the Open Project of State Key Laboratory of Special Vehicles and Their Drive System Intelligent Manufacturing, and the Tianjin University for Peiyang Elite Scholar (Grant no. 60301014).

REFERENCES

[1] A. Thakur, S. Chowdhury, P. Vec, C. Wang, W. Losert and S.K. Gupta, "Indirect pushing based automated micromanipulation of biological cells using optical tweezers," International Journal of Robotics Research, vol. 33, no. 8, pp. 1098-1111, 2014.

[2] H.C. Liaw and B. Shirinzadeh, "Robust adaptive constrained motion tracking control of piezo-actuated flexure-based mechanisms for micro/nano manipulation," IEEE Transactions on Industrial Electronics, vol. 58, no. 4, pp. 1406–1415, Apr. 2011.

[3] S. Zimmermann, T. Tiemerding and S. Fatikow, "Automated Robotic Manipulation of Individual Colloidal Particles Using Vision-Based Control," IEEE/ASME Transactions on Mechatronics, vol. 20, no. 5, pp. 2031-2038, Oct. 2014.

[4] E. Avci, K. Ohara, C.N. Nguyen, C. Theeravithayangkura, M. Kojima, T. Tanikawa, Y. Mae and T. Arai, "High-Speed Automated Manipulation of Microobjects Using A Two-Fingered Microhand," IEEE Transactions on Industrial Electronics, vol. 62, no. 2, pp. 1070-1079, Feb. 2014.

[5] C. Liang, F. Wang, Y. Tian, X. Zhao, H. Zhang, L. Cui, D. Zhang, and P. Ferreira, "A novel monolithic piezoelectric actuated flexure-mechanism based wire clamp for microelectronic device packaging," Review of Scientific Instruments, vol. 86, no. 4, pp. 045106, 2015.

[6] M. Rakotondrabe and I. A. Ivan, “Development and force/position control of a new hybrid thermo-piezoelectric microgripper dedicated to micromanipulation tasks,” IEEE Transactions on Automation Science and Engineering, vol. 8, no. 4, pp. 824-834, Oct. 2011.

[7] C. Liang, F. Wang, Y. Tian, X. Zhao, and D Zhang, “Development of a high speed and precision wire clamp with both position and force regulations,” Robotics and Computer-Integrated Manufacturing, vol.44, pp.208-217, 2017.

[8] N. Chronis, L.P. Lee, “Electrothermally activated SU-8 microgripper for single cell manipulation in solution,” Journal of Microelectromechanical Systems, vol. 14, no. 4, pp. 857-862, 2005.

[9] J. Park, S. Kim, D.H. Kim, B. Kim, S. Kwon, J.O. Parker and K.I. Lee “Identification and control of a sensorized microgripper for micromanipulation.” IEEE/ASME Transactions on Mechatronics, vol. 10, no. 5, pp. 601-606, Oct. 2005.

[10] Kyung J H, Ko B G, Ha Y H, et al. Design of a microgripper for micromanipulation of microcomponents using SMA wires and flexible hinges. Sensors & Actuators A Physical, 2008, 141(1):144-150.

[11] F. Wang, C. Liang, Y. Tian, X. Zhao, and D. Zhang, “Design of a piezoelectric-actuated microgripper with a three-stage flexure-based amplification,” IEEE/ASME Transactions on Mechatronics, vol. 20, no. 5, pp. 2205-2213, 2015.

[12] K. Cai, Y. Tian, F. Wang, D. Zhang and B. Shirinzadeh, “Development of a piezo-driven 3-DOF stage with T-shape flexible hinge mechanism,” Robotics and Computer-Integrated Manufacturing, vol. 37, pp. 125-138, 2016.

[13] W. Chen, X. Shi, W. Chen, and J. Zhang, “A two degree of freedom micro-gripper with grasping and rotating functions for optical fibers assembling,” Review of Scientific Instruments, vol. 84, no. 11, pp. 115111, 2013.

[14] Guo Z, Tian Y, Liu X, et al. An inverse Prandtl–Ishlinskii model based decoupling control methodology for a 3-DOF flexure-based mechanism. Sensors & Actuators A Physical, 2015, 230:52-62.

[15] X. Sun, W. Chen, Y. Tian, S. Fatikow, R. Zhou, J. Zhang and M. Mikczinski, "A novel flexure-based microgripper with double amplification mechanisms for micro/nano manipulation," Review of Scientific Instruments, vol. 84, no. 8, pp. 085002, 2013.

[16] Q. Xu, "A new compliant microgripper with integrated position and force sensing," IEEE/ASME International Conference on Advanced Intelligent Mechatronics, pp. 591-596, 2013.

[17] D.H. Wang, Q. Yang and H.M. Dong, "A monolithic compliant piezoelectric-driven microgripper: design, modeling, and testing," IEEE/ASME Trans. Mechatronics, vol. 18, no. 1, pp. 138-147, Feb. 2013.

[18] Zubir M N M, Shirinzadeh B. Development of a novel flexure based microgripper for precision manipulation of micro-objects. Sensors and Actuators A Physical, 2009, 150(2):257-266.

[19] H. Chaudhary, V. Panwar, R. Prasad and N. Sukavanam, "Adaptive neuro fuzzy based hybrid force/position control for an industrial robot manipulator," Journal of Intelligent Manufacturing, pp. 1-10, 2014.

[20] K. Rabenorosoa, C. Clevy, P. Lutz. "Hybrid force/position control applied to automated guiding tasks at the microscale," Proceedings of the IEEE/RSJ International Conference on Intelligent Robots and Systems, pp. 4366-4371, 2010.

[21] Q. Xu, "Precision position-force interaction control of a piezoelectric multimorph microgripper for microassembly," IEEE Transactions on Automation Science and Engineering, vol. 10, no. 3, pp. 503-514, July. 2013.

[22] Q. Xu, "Robust impedance control of a compliant microgripper for high-speed position-force regulation," IEEE Transactions on Industrial Electronics, vol. 62, no. 2, pp. 1201-1209, Feb. 2015.

[23] F. Wang, C. Liang, Y. Tian, X. Zhao and D. Zhang “Design and control of a compliant microgripper with a large amplification ratio for high-speed micro manipulation,” IEEE/ASME Transactions on Mechatronics, vol. 21, no. 3, pp. 1262-1271,Jan. 2016.

[24] Q. Xu, “Design and Smooth Position-force Switching Control of a Miniature Gripper for Automated Microhandling,” IEEE Transactions on Industrial Informatics, vol. 10, no. 2, pp. 1023-1032, May. 2014.

[25] F. Wang, X. Zhao, D. Zhang, Z. Ma and X. Jing. “Robust and precision control for a directly-driven XY table,” Proceedings of the Institution of Mechanical Engineers Part C Journal of Mechanical Engineering Science, vol. 225, no. 5, pp. 1107-1120, 2011.

[26] Q. Xu, M. Jia, “Model reference adaptive control with perturbation estimation for a micropositioning system,” IEEE Transactions on Control Systems Technology, vol. 22, no. 1, pp. 352-359, Mar. 2014.

[27] B.E. Helfrich, C. Lee, D. Bristow, X.H. Xiao, J. Dong, A.G. Alleyne, S.M. Salapaka and P.M. Ferreira, “Combined-feedback control and iterative learning control design with application to nanopositioning systems,” IEEE Transactions on Control Systems Technology, vol. 18, no. 2, pp. 336-351, July. 2010.

[28] Y. Li, Q. Xu, “Design and robust repetitive control of a new parallel-kinematic XY piezostage for micro/nanomanipulation,” IEEE/ASME Transactions on Mechatronics, vol. 17, no. 6, pp. 1120-1132, Dec. 2012.

[29] Y. Yang, Y.Wei, J. Lou., G. Tian, X. Zhao and L. Fu, “A new piezo-driven microgripper based on the double-rocker mechanism,” Smart Materials and Structures, vol. 24, no. 7, pp. 075031, 2015.

[30] Z. Long, J. Zhang, Y. Liu, C. Han, Y. Li and Z. Li, “Dynamics Modeling and Residual Vibration Control of a Piezoelectric Gripper During Wire Bonding,” IEEE Transactions on

Components, Packaging and Manufacturing Technology, July. 2017. DOI: 10.1109/TCPMT.2017.2723458.